Fernández-Martínez, A.B. et al. (2015) 'VIP induces NF-κB1-nuclear localisation through different signalling pathways in human tumour and non-tumour prostate cells', Cellular signalling, 27(2), pp. 236–244.

VIP induces NF-κB1-nuclear localisation through different signalling pathways in human tumour and non-tumour prostate cells

Ana B. Fernández-Martínez [a], María J. Carmena [a], Ana M. Bajo [a], Eva Vacas [a], Manuel Sánchez-Chapado [b,c], Juan C. Prieto [a,*]

[a] *Department of Systems Biology, Unit of Biochemistry and Molecular Biology, University of Alcalá, 28871 Alcalá de Henares, Spain*

[b] *Department of Surgery and Medical and Social Sciences, University of Alcalá, 28871 Alcalá de Henares, Spain*

[c] *Department of Urology, Príncipe de Asturias Hospital, 28871 Alcalá de Henares, Spain*

* Corresponding author. Tel.: +34 918854527; fax: +34 918854585.

E-mail address: juancarlos.prieto@uah.es (J.C. Prieto).

Abstract

The nuclear factor κB (NF-κB) is a powerful activator of angiogenesis, invasion and metastasis. Transactivation and nuclear localisation of NF-κB is an index of recurrence in prostate cancer. Vasoactive intestinal peptide (VIP) exerts similar effects in prostate cancer models involving increased expression of vascular endothelial growth factor (VEGF) and cyclooxygenase-2 (COX-2) which are related to NF-κB transactivation. Here we studied differential mechanisms of VIP-induced NF-κB transactivation in non-tumour RWPE-1 and tumour LNCaP and PC3 human prostate epithelial cells. Immunofluorescence studies showed that VIP increases translocation of the p50 subunit of NF-κB1 to the nucleus, an effect that was inhibited by curcumin. The signalling transduction pathways involved are different depending on cell transformation degree. In control cells (RWPE1), the effect is mediated by protein kinase A (PKA) activation and does not implicate extracellular signal-regulated kinase (ERK) or phosphoinositide 3-kinase (PI3-K) pathways whereas the opposite is true in tumour LNCaP and PC3 cells. Exchange protein directly activated by cAMP (EPAC) pathway is involved in transformed cells but not in control cells. Curcumin blocks the activating effect of VIP on COX-2 promoter/prostaglandin E_2 (PGE_2) production and VEGF expression and secretion. The study incorporates direct observation on COX-2 promoter and suggests that VIP effect on VEGF may be indirectly mediated by PGE_2 after being synthesised by COX-2, thus amplifying the initial signal. We show that the signalling involved in VIP effects on VEGF is cAMP/PKA in non-tumour cells and cAMP/EPAC/ERK/PI3K in tumour cells which coincides with pathways mediating p50 nuclear translocation. Thus, VIP appears to use different pathways for NF-κB1 (p50) transactivation in prostate epithelial cells depending on whether they are transformed or not. Transformed cells depend on pro-survival and pro-proliferative signalling pathways involving ERK, PI3-K and cAMP/EPAC which supports the potential therapeutic value

of these targets in prostate cancer.

Keywords: VIP; cAMP; NF-κB; PI3-K; Tumour prostate cells

Abbreviations

VIP, vasoactive intestinal peptide

EPAC, cAMP/exchange protein directly activated by cAMP

NF-κB, nuclear factor-κB

PKA, cAMP-dependent protein kinase

ERK, extracellular-signal regulated kinase

PI3-K, phosphoinositide 3-kinase

GEF, PKA- independent guanine nucleotide exchange factor

COX-2, cyclooxygenase-2

PGE_2, prostaglandin E_2

VEGF, vascular endothelial growth factor

MMP, metalloproteinase

RT-PCR, real-time quantitative PCR

1. Introduction

In Caucasian men, prostate cancer is the second most frequently diagnosed cancer and a leading cause of cancer death in the Western world [1]. Treatment of prostate cancer depends on its stage and currently includes surgery, radiotherapy, chemotherapy and androgen deprivation therapy. A large proportion of patients with advanced prostate cancer undergoing androgen deprivation therapy eventually develop hormone-refractory prostate cancer so that treatment is essentially palliative [2]. Systemic treatment of advanced or metastatic cancers is mainly carried out by chemotherapy. Targeted chemotherapy represents a modern and promising oncological strategy. Receptors for peptides hormones in tumour cells may serve as targets for peptide ligands bound to cytotoxic agents.

The nuclear factor-κB (NF-κB) family of transcription factors has been shown to be constitutively activated in various human malignancies, including leukaemias, lymphomas, and a number of solid tumours. Constitutive activation of NF-κB has been detected in androgen-independent prostate cancer cell lines as well as in prostate cancer tissue [3–7]. NF-κB may promote cell growth and proliferation in prostate cancer cells by regulating expression of genes such as c-myc, cyclin D1, and interleukin-6 (IL-6). NF-κB may also inhibit apoptosis in prostate cancer cells through activation of expression of anti-apoptotic genes, such as Bcl-2, although pro-apoptotic activity of NF-κB has also been reported [8]. NF-κB-mediated expression of genes involved in angiogenesis (IL-8, vascular endothelial growth factor VEGF), and invasion and metastasis (metalloproteinase 9 MMP9, urokinase plasminogen activator uPA, uPA receptor uPAR) may further contribute to the progression of prostate cancer [9]. Induction of miR-221/222 transcription has been recently proposed as an additional mechanism through which NF-κB and c-Jun, two transcription factors deeply involved in prostate cancer

onset and progression, contribute to oncogenesis [10]. Inactive NF-κB is located in the cytoplasm of all cells in resting state and it can be activated and translocated to the nucleus resulting in a sequence of events. NF-κB functions as a hetero- or homo-dimer, the most studied dimer being p50:p65 which is activated by the canonical pathway. Activation and nuclear translocation of NF-κB dimers occur through a signal transduction pathway involving different kinases. Blockade of NF-κB activity in human prostate carcinoma cells is associated with suppression of angiogenesis, invasion, and metastasis [11,12]. Vasoactive intestinal peptide (VIP) is a neuropeptide with a wide range of biological effects [13] which are mediated by VIP receptors, VPAC1 and VPAC2. They belong to the class II family of G-coupled protein receptors and the initial effect of VPAC1 or VPAC2 binding to VIP is mainly the increase of cyclic AMP [14]. In human prostate cancer cells, VIP increases the expression of the major angiogenic factor, VEGF, and the proinflammatory enzyme cyclooxygenase-2 (COX-2) [15,16], stimulates epidermal growth factor receptor 2 (HER2) phosphorylation [17], and promotes metastatic progression [18]. VIP is also able to transform control epithelial cells into cells capable of inducing tumours in mice [19]. All these effects of VIP in prostate are mediated by transactivation of NF-κB and inhibited by the antioxidant curcumin. Furthermore, curcumin demonstrated anti-tumour activity in androgen deprivation-resistant prostate cancer xenografts [20]. In addition, the neuropeptide induces neuroendocrine differentiation in androgen- dependent prostate cancer LNCaP cells through protein kinase A (PKA), Ras, mitogen-activated protein kinase (MAPK) and phosphatidyl inositol 3-kinase (PI3-K) [21,22].

In this study, the effect of VIP on the transactivation of NF-κB1 in human tumour and non-tumour prostate cells was investigated in order to better determine the intracellular signals involved in the mechanisms of VIP action in the prostate gland and to identify additional targets with potential therapeutic value.

2. Materials and methods

2.1. Cell lines and culture

Non-neoplastic human prostatic epithelial cells (RWPE-1) as well as androgen-dependent (LNCaP, originated from a lymph node metastasis) and androgen-independent (PC3, derived from a bone metastasis) prostatic carcinoma cells, which exhibit different features of prostate cancer progression, were used in receptor expression analysis. Other studies were performed in PC3 cells. The three cell lines were obtained from the American Type Culture Collection (Manassas, VA, USA). RWPE-1 cells were maintained in complete keratinocyte serum-free medium (K-SFM) containing 50 μg/mL bovine pituitary extract and 5 ng/mL EGF. LNCaP and PC-3 cells were cultured in RPMI-1640 medium (Life Technologies, Barcelona, Spain) supplemented with 1% antibiotic/ antimycotic and 10% foetal bovine serum (FBS). The cells were grown at 37 °C in a humidified 95% air/5% carbon dioxide atmosphere and split weekly with 0.5% trypsin/0.02% EDTA. All culture media components were purchased from Invitrogen (Barcelona, Spain).

2.2. Confocal immunofluorescence microscopy

Cells were cultured on glass coverslips. The coverslips were fixed and permeabilised with methanol at −20 °C for 15 min and incubated in 4% bovine serum albumin (BSA) in PBS at room temperature for 1 h. The coverslips were incubated with rabbit anti-$VPAC_1$ and $VPAC_2$ receptors (working dilution 1:2000) or anti-p50 (1:50) antibodies (Affinity Bioreagents, Golden, CO, USA) for 1 h at room temperature. After washing with PBS, coverslips were incubated with goat anti-rabbit FITC-conjugated secondary antibody (1:2000) (Alexa, Invitrogen, Barcelona, Spain) for 1 h. Cells were washed again in PBS and mounted in aqueous antifade medium followed by analyses with a Leica TCS-SL confocal laser scan microscope.

2.3. Isolation of subcellular fractions and Western blotting

Subcellular fractions were essentially obtained as described previously [23]. Cultured cells were washed twice with ice-cold PBS and then harvested, scraped into ice-cold PBS, and pelleted by centrifugation at 500 ×*g* for 5 min at 4 °C. To get cellular lysates, the cells were kept on ice for 30 min in a solution containing 20 mM Tris–HCl (pH 7.5), 1 mM EDTA, 0.5 M NaCl, 0.5% Nonidet NP-40, 2 mM phenylmethylsulphonylfluoride (PMSF), and 10 μg/mL protease inhibitors. Thereafter, they were pelleted by centrifugation at 4000 ×*g* for 5 min at 4 °C. The cytosolic and nuclear contents were extracted with a commercially available kit according to the manufacturer's instructions (BD Bioscience, Madrid, Spain). In another context, isolation of plasma membranes was performed by centrifugation of cell lysates at 800 ×*g* for 20 min at 4 °C, followed by centrifugation of the supernatant at 100,000 ×*g* for 20 min at 4 °C; the pellet corresponded to the plasma membranes. Protein content was measured by the Bradford assay using BSA as a standard. Protein (30 μg) was solubilised in 50 mM Tris–HCl buffer (pH 6.8) containing 10% (v/v) glycerol, 3% (w/v) SDS, 0.01% bromophenol blue, and 0.7 M β-mercaptoethanol, and then heated at 95 °C for 5 min. Proteins were resolved by 10% SDS-PAGE, and then transferred to nitrocellulose sheets (BioTrace/NT, Pall Corporation, East Hills, NY, USA). Blots were incubated with the primary antibodies against $VPAC_1$ and $VPAC_2$ receptors at dilutions recommended for 1 h at room temperature according to the manufacturer's instructions. After treatment for 1 h at room temperature with the corresponding HRP-labelled secondary antiserum (1:4000) (BD Biosciences), the signals were detected with enhanced chemiluminescence reagent (Amersham, Uppsala, Sweden) using anti-β-actin antibody (1:10,000) (Merck, Darmstadt, Germany) for loading control.

2.4. Cyclic AMP measurement

The stimulatory effect of VIP on cAMP levels was determined in human prostate epithelial

cells: RWPE-1 (600,000 cells), LNCaP (400,000 cells) and PC3 (250,000 cells) were placed in 6-well plates and treated with 0.75 mL of medium containing 1% BSA, 1 mg/mL bacitracin, 0.05 mM phenylmethylsulphonylfluoride (PMSF) and 0.4 mM 3-isobutyl-1-methylxanthine (IBMX, a non-selective phosphodiesterase inhibitor which attenuates cAMP breakdown in order to assess primarily cAMP generation). After 30 min of treatment, the medium was removed, 70% ethanol was added and then well contents were transferred to fresh tubes and evaporated at 60 °C. Dried samples were dissolved in 0.2 M phosphate buffer and stored at −20 °C until further assays. Measurement of cAMP levels was carried out by means of a competitive binding assay [24].

2.5. Single-step real-time quantitative PCR

Total cell RNA was isolated from prostate cells with TriReagent (Sigma, Alcobendas, Spain) and real-time quantitative RT-PCR analysis was performed in 2 ng samples using SYBR Green PCR master mix (Life Technologies, Barcelona, Spain) and a one-step RT-PCR protocol as previously described [24]. Primer sequences for genes were as fol- lows (sequences 5′–3′): $VEGF_{165}$ sense: GACAAGAAAATCCCTGTGGG CAAC and antisense: GCGAGTCTGTGTTTTTGC; β-actin sense: AGAAGG ATTCCTATGTGGGCG and antisense: CATGTC CCAGTTGGTGAC.

2.6. Quantification of PGE_2 and VEGF

RWPE-1, LNCaP and PC3 cell lines, were placed in 100-mm cell culture dishes at a density of 2.5×10^6 cells in complete medium for 24 h. Controls received medium only. The supernatants were stored at −80 °C for further assays. PGE_2 and VEGF levels in the secreted medium were determined by ELISA with commercially available kits according to the manufacturer's instructions (Cayman, Ann Arbor, Michigan, USA) (R&D Systems, Minneapolis, MN, USA).

2.7. Transient transfection and luciferase assay

Transient transfection was performed with luciferase plasmid phPES2 reporter containing the promoter fragment −327 to +59, a gift from Dr. Hiroyasu Inoue (Nara Women's University, Nara, Japan). Cells (2.5×10^5 cells per well) were plated in 6-well plates 24 h before transfection. Thereafter, cells were incubated for 5 h at 37 °C with 1 mL OptiMEM (Invitrogen) containing 5 μL lipofectamine (Invitrogen), 1 μg human phPES2 reporter and 1 μg renilla luciferase reporter as an internal control. Transfected cells were incubated with complete growth medium for 24 h and then treated with 0.1 μM VIP for 6 h. Finally, firefly luciferase activity of the construct reporter was measured with a Lumat LB9506 luminometer (Berthold Technologies, Herts, UK) and normalised against the renilla luciferase activity by using the dual-luciferase reporter assay system (Promega, Madison, WI, USA).

2.8. Statistical analysis

Each experiment was repeated at least three times. Results are expressed as the mean ± S.E.M. Statistical analysis was performed by a nonparametric Bonferroni's test for multiple comparisons after one or two-way analysis of variance (ANOVA); p b 0.05 was considered statistically significant.

3. Results

3.1. Localisation of VIP receptors

The emerging paradigm of the localisation of GPCRs not only in plasma membrane but also in intracellular compartments was studied for VIP receptors by confocal fluorescence microscopy (Fig. 1). The inclusion of a negative control showed the absence of unspecific fluorescence. Specific immunodetection revealed a differential pattern of expression of VIP receptor subclasses. Thus, $VPAC_2$ receptor staining was identified on plasma membrane and cytosol. However, $VPAC_1$ receptor staining was found on the nuclear envelope of the three prostate cell lines studied. The use of subcellular fractions allowed us to identify by means of Western-blotting the differential distribution of VIP-receptor proteins in plasma membrane, cytosol and nucleus from the three cell lines studied (Fig. 1).

3.2. Cyclic AMP production

The functionality of VIP receptors in the non-neoplastic human prostate cell line, RWPE-1, was assessed by the ability of VIP to stimulate adenylate cyclase activity (Fig. 2). As commented in Materials and methods, the non-selective phosphodiesterase inhibitor IBMX was included in assays so as to attenuate cAMP breakdown and thus assess primarily cAMP generation. The study was performed in parallel with two human prostate cancer cell lines, LNCaP and PC3, which represent two stages of the androgen dependence of the disease. The neuropeptide duplicated the cAMP basal levels in RWPE-1 cells at low peptide concentration. In cancer cell lines, the response was dose-dependent and quantitatively similar although basal cAMP levels were higher in PC3 cells. VIP treatment resulted in maximal cAMP levels in LNCaP and PC3 cells that were about 25 times higher than those reached in RWPE-1 cells.

3.3. Effect of VIP and curcumin on p50 nuclear transactivation

We checked by means of confocal microscopy if the inhibitory activity of the pigment

curcumin on VIP effects directly involves NFκB. For this purpose, cells were incubated with 0.1 mM VIP and/or 10 mM curcumin and p50 nuclear translocation was observed (Fig. 3). The immunofluorescence images and the corresponding quantification showed that curcumin completely abolished this effect of VIP in the three cell lines considered.

3.4. Pathways involved in NF-κB1 transactivation

While cAMP signalling has classically been associated with the acti- vation of PKA, many effects of VIP do not rely solely upon PKA signalling. In this context, cAMP also directly regulates the exchange protein directly activated by cAMP (EPAC), a guanine nucleotide exchange factor that is a crucial mediator of PKA-independent cAMP signalling [25]. To check the signal transduction pathways involved in VIP-induced p50 nuclear translocation, RWPE-1, LNCaP and PC3 cells were treated with 0.1 μM VIP and/or specific inhibitors of PKA (10 μM H89), ERK1/2 (10 μM PD98059), and PI3K (0.1 μM wortmannin) or an activator of the EPAC pathway (0.3 mM O-CPT-2Met cAMP) and observed by immunofluorescence microscopy (Fig. 4). The analysis of the emitted fluorescence reveals that in control epithelial cells, RWPE1, VIP effect is mediated by activation of cAMP-dependent protein kinase (PKA) and it implicates neither ERK1/2 nor PI3K pathways as it occurs in tumour cells, LNCaP and PC3. The PKA-independent guanine nucleotide ex-change factor (GEF)/EPAC pathway is involved in VIP effects in trans- formed cells but not in non-tumoural cells. The pathway involved is cAMP/EPAC/PI3K in LNCaP cells whereas PC3 cells use cAMP/PKA, EPAC/ERK and PI3K pathways.

3.5. Effect of VIP on COX-2 promoter activity and PGE_2 secretion

Previous observations from our laboratory showed by means of immunodetection assays that VIP increases COX-2 protein levels in prostate cell lines [16]. In the present study, we analysed the effects of VIP on the luciferase activity of a pCOX-2-Luc construct. Results showed

that VIP increased the activity of the construct in the three cell lines whereas curcumin treatment abolished this effect (Fig. 5). It suggests that NF-κB was involved in the effect of VIP upon COX-2 levels.

In order to investigate whether VIP-increased expression of COX-2 protein was accompanied by enhancement of PGE_2 secretion, an ELISA was carried out with RWPE-1, LNCaP and PC3 cell lines. PGE_2 protein levels were measured in the extracellular culture medium of these prostate epithelial cell lines after treatment with 0.1 μM VIP for 8–12 h. Results (Fig. 5, inset) indicate that PGE_2 levels were maximal at 8–12 h in RWPE-1 cells and 4–6 h in cancer cells. Thus, the increase of COX-2 levels by VIP was accompanied by enhancement of PGE_2 levels. In addition to this, we measured $VEGF_{165}$ levels in the medium of the cell lines treated with 10 μM PGE_2. The results indicated that $VEGF_{165}$ levels increased by PGE_2-treatment up to 48 h in all cell lines as compared to untreated cells. The fastest and highest response was seen in PC3 cells.

Fig. 5B incorporates all the inhibitors used in the present study in order to define the pathway of activation of COX-2 promoter by VIP. RWPE-1, LNCaP and PC3 cells were treated with 0.1 μM VIP and/or specific inhibitors of PKA (10 μM H89), ERK1/2 (10 μM PD98059), and PI3K (0.1 μM wortmannin) or an activator of the EPAC pathway (0.3 mM O-CPT-2Met cAMP).

3.6. Effect of PGE_2 on VEGF secretion

In order to study the effect of PGE_2 on VEGF secretion, RWPE-1, LNCaP and PC3 cell lines were incubated with 1 mM PGE_2 and $VEGF_{165}$ levels were measured in the extracellular medium by ELISA. As shown in Fig. 6, a significant response was seen in the three classes of cells as compared with untreated controls.

3.7. Effect of VIP on VEGF expression and secretion

With the purpose of checking if the effect of VIP on PGE_2 secretion was accompanied by an enhancement in $VEGF_{165}$ protein production, RWPE-1, LNCaP and PC3 cells were treated with VIP, and $VEGF_{165}$ pro- duction and expression were analysed by real-time RT-PCR (Fig. 7A) or ELISA (Fig. 7B), respectively. The results showed that 0.1 μM VIP in- creased both $VEGF_{165}$ production and mRNA expression in the three cell lines. Cell treatment with curcumin abolished the VIP effect, thus involving NF-κB activity in VIP stimulation of $VEGF_{165}$ expression and production. Furthermore, we used a specific inhibitor of p50-subunit nuclear transport to study VEGF production in the three cell lines after VIP treatment in the absence or presence of that inhibitor (50 μM sc-3060, Santa Cruz Biotechnology, Dallas, TX, USA). In this manner, we could confirm the involvement of NF-κB in VEGF regulation by VIP. The corresponding results appear as an inset in Fig. 7.

3.8. Pathways involved in $VEGF_{165}$ production

In order to check the signal transduction pathways involved in VIP- induced VEGF secretion, RWPE-1, LNCaP and PC3 cells were treated with 0.1 μM VIP and/or specific inhibitors of PKA (10 μM H89), ERK1/2 (10 μM PD98059), and PI3K (0.1 μM wortmannin) or an activator of EPAC pathway (0.3 mM O-CPT-2Met cAMP). Measurement of $VEGF_{165}$ levels by ELISA (Fig. 7C) indicated that the pathways involved in this effect are the same seen in p50 translocation in the three cell lines.

4. Discussion

The role of VIP in different events of prostate cancer has been extensively studied by our laboratory using both cells and tissue samples. Indeed, we observed the ability of VIP to transform a normal epithelial phenotype towards tumour characteristics [19]. The present investigation adds new observations to this aspect and provides information on the behaviour of VIP receptor/effector and its effects in non-neoplastic RWPE-1 cells and shows that the

signalling pathways moved for these purposes are different from those used in tumour cells.

Regarding the cellular localisation of specific VIP receptors, confocal microscopy studies using specific antibodies for $VPAC_1$ or $VPAC_2$ receptors showed a nuclear localisation for $VPAC_1$ receptors. This observation has been also pointed out recently in prostate and breast cancer cells [23,26]. It provides evidence for a novel intracrine mode of genomic regulation by endogenously-produced VIP and/or nuclear translocation of peripheral $VPAC_1$ receptors. Western-blot analysis of subcellular fractions served to identify the presence of both VIP receptor subclasses in plasma membrane, cytosol and nucleus from the three cell lines studied. It supports the idea that VPAC receptors are a dynamic system for signalling from plasma membrane and nuclear membrane complex.

In the current study, we explored the mechanism of VIP-induced NF-κB activation in human prostate normal and tumour cells. We ob- served that VIP activates the classic NF-κB pathway through different mechanisms that involve cAMP. NF-κB is a powerful activator of the malignant state and exerts this function by regulating the transcription of genes encoding many mediators important for energy metabolism, cell proliferation, survival and angiogenesis [27,28]. NF-κB is intrinsically activated in androgen-independent prostate cancer cell lines as well as in prostate cancer tissues [3,29–31]. Moreover, blocking of NF-κB/relA activity in human prostate cancer cells is associated with suppression of angiogenesis, invasion and metastasis [32]. It has been also described that nuclear localisation of NF-κB is predictive of biochemical recurrence in patients with positive margin prostate cancer [33]. Confocal microscopy served us to observe that VIP induced NF-κB1 translocation in the three prostate cell lines, but the signalling pathways and molecular effectors involved were different from each other. In non-neoplastic RWPE-1 cells, VIP stimulates cAMP production whose activation results in p50 nuclear localisation. In tumour cells, PKA-independent/EPAC pathway is involved and triggers the activation of ERK and

PI3K. However, androgen-dependent LNCaP and androgen-independent PC3 prostate cancer cells differ in that the second cell line uses both PKA and EPAC routes. Any type of cancer is associated with deregulation of as many as 500 different genes and characterised by the deregulation of cell signalling pathways at multiple steps leading to cancer phenotype. It is an accepted fact that the signalling pathways in tumour cells are very different from those in normal cells from which they are de- rived, affording opportunities for selective targeting in cancer treatment or prevention.

Curcumin, a yellow-pigment substance and component of turmeric (*Curcuma longa*), was identified more than a century ago. Curcumin possesses a great potentiality for being used in cancer chemotherapy because of its control over the machineries of cell survival, proliferation, invasion, and angiogenesis. The mechanisms implicated are diverse and appear to involve a combination of cell signalling pathways at multiple levels [33]. We noted here that curcumin blocked NF-κB through the inhibition of nuclear translocation of NF-κB p50 subunit and inhibited the activating effect of VIP on COX-2 promoter and VEGF expression and secretion. In a previous work, we reported that curcumin abrogated VIP-induced COX-2 expression in non-neoplastic and cancer prostate cells, which supports again the involvement of NF-κB in such effect; moreover, these responses were accelerated with cancer status progression [16]. The present investigation incorporates direct observation on COX-2 promoter and suggests that the effect of VIP on VEGF may be indirectly mediated by increased PGE_2 levels related to COX-2 mediated synthesis, amplifying the initial signal previously observed in LNCaP cells by our laboratory [15]. Also, we found that VIP treatment stimulates its own synthesis, so that exogenous VIP could be responsible for the earlier VEGF response and both endogenous VIP and PGE_2 could contribute to its maintenance (data not shown). Finally, present data show that the signalling involved in these effects on VEGF are conceivably cAMP/PKA in control cells and

cAMP/EPAC/ERK/PI3K in tumour cells, which is coincident with the pathways involved in p50 nuclear translocation.

5. Conclusions

This study shows that VIP induces p50 nuclear translocation in human tumour and non-tumour prostate epithelial cells by different signalling pathways. Moreover, curcumin suppresses nuclear localization of p50 and all VIP effects mediated by p50 (COX-2/PGE_2 and VEGF). These observations together with previous data showing the inhibitory effects of curcumin and COX-2 inhibitor, NS398, in an animal model bearing tumour xenografts [19] greatly support that NF-κB1 could be an important prognostic marker in prostate cancer and should be studied further pointing to this objective in a large sample of patients.

Disclosure/conflict of interest

There are no conflicting interests. All the authors have approved the final article.

Author contribution

Fernández-Martínez and Vacas performed lab work as partial fulfilment of their Ph.D. theses. Sánchez-Chapado provided consultation; Carmena and Bajo designed all experiments and analysed the results; Prieto coordinated the investigation and wrote the paper.

Acknowledgements

Grant support: This work was financially supported by the Ministerio de Ciencia e Innovación (grant SAF2007-63794). A.B.F.M. was a fellow of the University of Alcalá.

References

[1] R. Siegel, J. Ma, Z. Zou, A. Jemal, CA Cancer J. Clin. 64 (2014) 9–29.

[2] M.J. Morris, H.I. Scher, Cancer 89 (2000) 1329–1348.

[3] C.D. Chen, C.L. Sawyers, Mol. Cell. Biol. 22 (2002) 2862–2870.

[4] J. Suh, F. Payvandi, L.C. Edelstein, P.S. Amenta, W.X. Zong, C. Gélinas, A.B. Rabson, Prostate 52 (2002) 183–200.

[5] J.S. Ross, B.V. Kallakury, C.E. Sheehan, H.A. Fisher, R.P. Kaufman Jr., P. Kaur, K. Gray, B. Stringer, Clin. Cancer Res. 10 (2004) 2466–2472.

[6] S. Shukla, G.T. MacLennan, P. Fu, J. Patel, S.R. Marengo, M.I. Resnick, S. Gupta, Neoplasia 6 (2004) 390–400.

[7] I.H. Koumakpayi, C. Le Page, A.M. Mes-Masson, F. Saad, Br. J. Cancer 102 (2010) 1163–1173.

[8] G. Jain, M.V. Cronauer, M. Schrader, P. Möller, R.B. Marienfeld, World J. Urol. 30 (2012) 303–310.

[9] J. Min, A. Zaslavsky, G. Fedele, S.K. McLaughlin, E.E. Reczek, T. De Raedt, I. Guney, D.E. Strochlic, L.E. MacConaill, R. Beroukhim, R.T. Bronson, S. Ryeom, W.C. Hahn, M. Loda, K. Cichowski, Nat. Med. 16 (2010) 286–294.

[10] S. Galardi, N. Mercatelli, M.G. Farace, S.A. Ciafrè, Nucleic Acids Res. 39 (2011) 3892–3902.

[11] S. Huang, C.A. Pettaway, H. Uehara, C.D. Bucana, I.J. Fidler, Oncogene 20 (2001) 4188–4197.

[12] A.D. Sanlioglu, I.T. Koksal, B. Karacay, M. Baykara, G. Luleci, S. Sanlioglu, Cancer Gene Ther. 13 (2006) 21–31.

[13] T.W. Moody, T. Ito, N. Osefo, R.T. Jensen, Curr. Opin. Endocrinol. Diabetes Obes. 18 (2011) 61–67.

[14] L.C. Racusen, H.J. Binder, Gastroenterology 73 (1977) 790–796.

[15] B. Collado, I. Gutiérrez-Cañas, N. Rodríguez-Henche, J.C. Prieto, M.J. Carmena, Regul. Pept. 119 (2004) 69–75.

[16] A.B. Fernández-Martínez, B. Collado, A.M. Bajo, M. Sánchez-Chapado, J.C. Prieto, M.J. Carmena, Mol. Cell. Endocrinol. 270 (2007) 8–16.

[17] S. Sotomayor, M.J. Carmena, A.V. Schally, J.L. Varga, M. Sánchez-Chapado, J.C. Prieto, A.M. Bajo, Int. J. Oncol. 31 (2007) 1223–1230.

[18]A.B. Fernández-Martinez, A.M. Bajo, M. Sánchez-Chapado, J.C. Prieto, M.J. Carmena, Prostate 63 (2009) 774–786.

[19]A.B. Fernández-Martínez, A.M. Bajo, M.I. Arenas, M. Sánchez-Chapado, J.C. Prieto, M.J. Carmena, Cancer Lett. 299 (2010) 11–21.

[20] A.B. Fernández-Martínez, A.M. Bajo, A. Valdehita, M.I. Arenas, M. Sánchez-Chapado, M.J. Carmena, J.C. Prieto, Peptides 30 (2009) 2357–2364.

[21]I. Gutiérrez-Cañas, N. Rodríguez-Henche, O. Bolaños, M.J. Carmena, J.C. Prieto, M.G. Juarranz, Br. J. Pharmacol. 139 (2003) 1050–1058.

[22] I. Gutiérrez-Cañas, M.G. Juarranz, B. Collado, N. Rodríguez-Henche, A. Chiloeches, J.C. Prieto, M.J. Carmena, Prostate 63 (2005) 44–55.

[23] A. Valdehita, A.M. Bajo, A.B. Fernández-Martínez, M.I. Arenas, E. Vacas, P. Valenzuela, A. Ruíz-Villaespesa, J.C. Prieto, M.J. Carmena, Peptides 31 (2010) 2035–2045.

[24] A.G. Gilman, Proc. Natl. Acad. Sci. U. S. A. 67 (1970) 305–312.

[25] N. El Zein, B. Badran, E. Sariban, J. Leukoc. Biol. (2008) 972–981.

[26]A.B. Fernández-Martínez, M.J. Carmena, M.I. Arenas, A.M. Bajo, J.C. Prieto, M. Sánchez-Chapado, Histol. Histopathol. 27 (2012) 1093–1101.

[27] M.S. Hayden, S. Ghosh, Gen. Dev. 26 (2013) 203–234.

[28]M. Moretti, J. Bennet, L. Tornatore, A.K. Thotakura, G. Franzoso, Int. J. Biochem. Cell Biol. 44 (2012) 2238–2243.

[29] S.T. Palayoor, M.Y. Youmell, S.K. Calderwood, C.N. Coleman, B.D. Price, Oncogene 18 (1999) 7389–7394.

[30]A.V. Gasparian, Y.J. Yao, D. Kowalczyk, L.A. Lyakh, A. Karseladze, T.J. Slaga, I.V. Budunova, J. Cell Sci. 115 (2002) 141–151.

[31]L. Lessard, A.M. Mes-Masson, L. Lamarre, L.L. Wall, J.B. Lattouf, F. Saad, BJU Int. 91 (2003) 417–420.

[32]S. Huang, C.A. Pettaway, H. Uehara, C.D. Bucana, I.J. Fidler, Oncogene 20 (2001) 4188–4197.

[33] V. Fradet, L. Lessard, L.R. Bégin, P. Karakiewicz, A.M. Masson, F. Saad, Clin. Cancer Res. 10 (2004) 8460–8464.

Figure legends

Fig. 1. Localisation of VIP receptors. Confocal immunofluorescence microscopy (upper panel): RWPE-1, LNCaP and PC3 human prostate cell lines were fixed, permeabilised and blocked. Then, they were incubated with anti-$VPAC_1$-receptor or anti-$VPAC_2$-receptor antibodies and thereafter with secondary antibody. The inclusion of a negative control shows the absence of unspecific fluorescence. All experiments were repeated three times and a representative photograph from each experiment is shown. Western-blotting (lower panel): subcellular fractions (plasma membrane, cytosol and nucleus) were analysed to identify VIP receptor subclasses in the three cell lines studied using β-actin as a loading control: a representative experiment is shown.

Fig. 2. Cyclic AMP production. The functionality of VIP receptors in prostate cell lines was assessed by the ability of the neuropeptide on the production of cAMP. RWPE-1, LNCaP and PC3 cells were stimulated by different doses of VIP for 30 min, and cAMP levels were measured as described under Section 2.3. Data are the mean ± S.E.M. ANOVA/Bonferroni's test,* $p < 0.05$; **$p < 0.01$, ***$p < 0.001$ vs. untreated cells (* to RWPE; $^{\#}$ to LNCaP; $^{+}$ to PC3). The EC_{50} value for each cell line appears under the graphic.

Fig. 3. Effect of VIP and curcumin on p50 nuclear transactivation. After pre-treatment for 1 h in the presence or absence of 10 mM curcumin, cells were stimulated for 6 h (RWPE-1), 1 h (LNCaP) or 45 min (PC3) with 0.1 μM VIP. Thereafter, cells were fixed, permeabilised and blocked. Then, the expression and localisation of p50 was analysed by confocal immunofluorescence as described under Section 2.2. All experiments were repeated three times and a representative photograph from each experiment is shown. The bar diagrams represent the mean ± S.E.M. *$p < 0.05$ or ***$p < 0.001$ vs. control group; $^{++}$ $p < 0.01$ or $^{+++}$ $p < 0.001$ vs. VIP.

Fig. 4. Pathways involved in NF-κB1 transactivation. A) RWPE-1, LNCaP and PC3 cell lines were pretreated with H89 (15 min) and incubated with O-CPT-2Me-cAMP or VIP. Then, the ex- pression and localisation of p50 was analysed by confocal immunofluorescence as described under Section 2.2. B) Prostate cell lines were pre-incubated with wortmannin (30 min) or PD98059 (1 h) and then, they were treated with 0.1 mM VIP. The expression and localisation of p50 was analysed by confocal immunofluorescence microscopy as described under Section 2.2. All experiments were repeated three times and a representative photograph from each experiment is shown. Each bar represents the fluorescence analysis and was expressed as arbitrary. Data are the mean ± S.E.M. ANOVA/Bonferroni's test *** $p < 0.001$ vs. untreated cells; $^{++}$ $p < 0.01$ vs. VIP.

Fig. 5. Effect of VIP on COX-2 promoter activity and PGE_2 secretion. Luciferase activity in lysates of cells which were transiently transfected with the pCOX-2-Luc. After transfection, cells were pretreated with curcumin (A) or H89, wortmannin or PD98059 (B) for 1 h and incubated with O-CPT-2Met-cAMP or VIP. The luciferase activity of the construct reporter was measured. Each bar represents the luciferase activity normalised by the Renilla luciferase activity and expressed as relative luminescence units (RLU). Data are the mean ± S.E.M. ANOVA/ Bonferroni test, ** $p < 0.01$; *** $p < 0.001$ vs. control and $^{+}$ $p < 0.05$; $^{++}$ $p < 0.01$ vs. $^{+++}$ $p < 0.001$ vs. VIP. Inset: Effect of VIP on extracellular PGE_2 levels in RWPE-1, LNCaP and PC3 cell lines. After incubation at the indicated times in the absence or presence of 0.1 μM VIP, culture media were taken and PGE_2 levels were measured by E.I.A. Data are the mean ± S.E.M. ANOVA/Bonferroni test, * $p < 0.05$ or ** $p < 0.01$ vs. control group.

Fig. 6. Effect of PGE_2 on VEGF secretion. RWPE-1, LNCaP and PC3 cell lines were incubated with 1 mM PGE_2 at the indicated times and VEGF-A levels in the extracellular medium were measured by ELISA. Results correspond to the mean ± S.E.M. and are representative of

at least three independent experiments, * $p < 0.05$ vs. untreated cells.

Fig. 7. Effect of VIP on VEGF expression and secretion. Prostate cell lines were pre-treated for 1 h with 10 mM curcumin and then, stimulated with 0.1 μM VIP. Total cell RNA was extracted and VEGF mRNA levels were measured by Q-RT-PCR (A) and VEGF-A levels in the extracellular medium were measured by ELISA (B). Inset: RWPE-1, LNCaP and PC3 cell lines were pretreated with a NF-κB inhibitor, sc-3060 (50 μM) for 1 h, and then incubated with VIP and the VEGF production measured by ELISA. C) Pathways involved in $VEGF_{165}$ production: RWPE-1, LNCaP and PC3 cell lines were pre-incubated with H89 (15 min), wortmannin (30 min) or PD98059 (1 h) and then, cells were incubated with O-CPT-2Met-cAMP or VIP at the indicated times. VEGF-A levels in the extracellular medium were measured by ELISA. Data are the mean ± S.E.M. ANOVA/Bonferroni test, ** $p < 0.01$; *** $p < 0.001$ vs. control, and $^{++}$ $p < 0.01$, $^{+++}$ $p < 0.001$ vs. VIP.

Figure 1

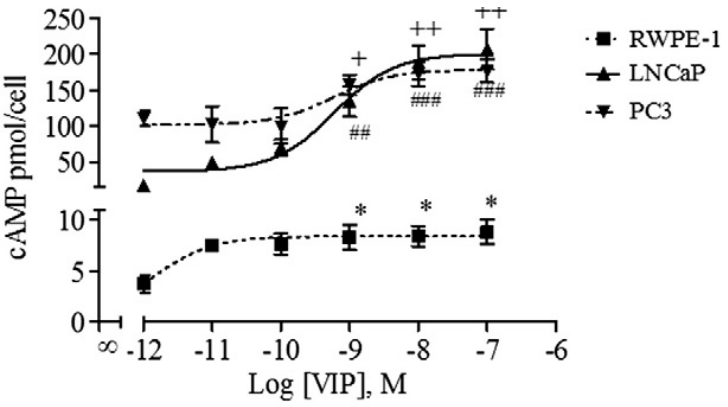

	RWPE-1	LNCaP	PC3
EC50	1.347e-012	6.003e-010	5.937e-010

Figure 2

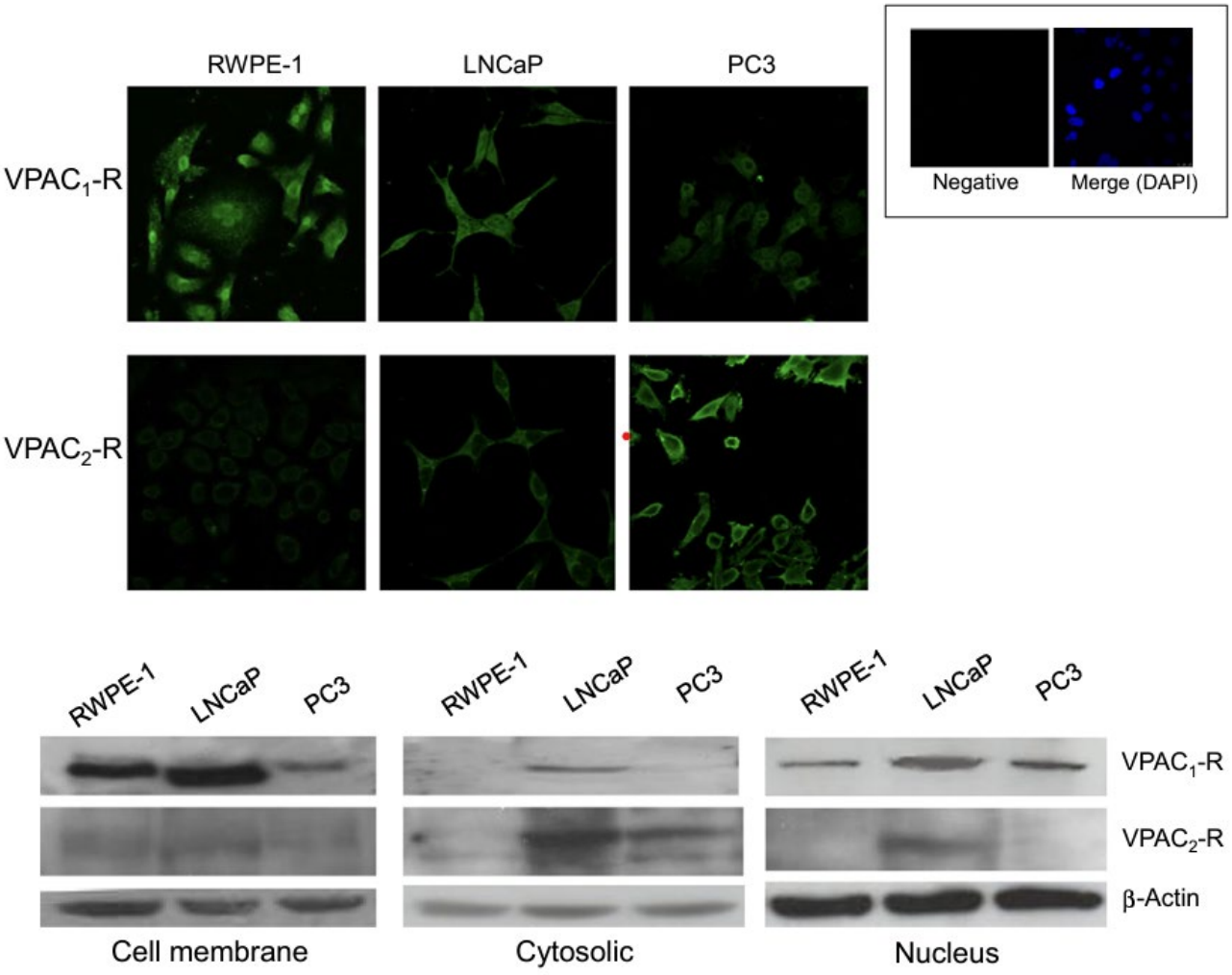
RWPE-1
LNCaP
PC3
VPAC1-R
VPAC2-R
Negative
Merge (DAPI)
RWPE-1
LNCaP
PC3
RWPE-1
LNCaP
PC3
RWPE-1
LNCaP
PC3
VPAC1-R
VPAC2-R
β-Actin
Cell membrane
Cytosolic
Nucleus

Figure 3

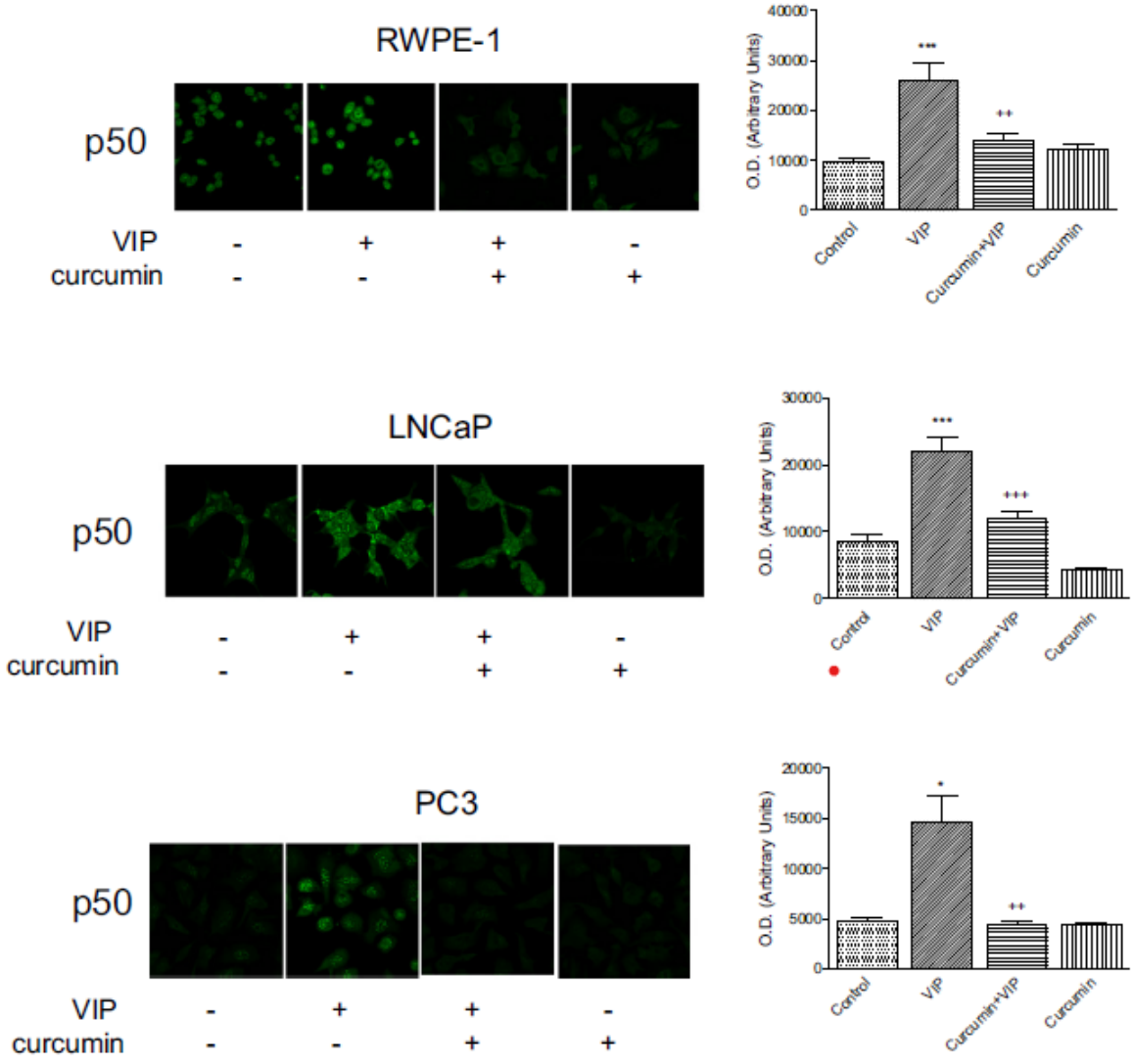
RWPE-1
p50
VIP - + + -
curcumin - - + +
O.D. (Arbitrary Units)
40000
30000
20000
10000
0
***
++
Control
VIP
Curcumin+VIP
Curcumin
LNCaP
p50
VIP - + + -
curcumin - - + +
O.D. (Arbitrary Units)
30000
20000
10000
0
***
+++
Control
VIP
Curcumin+VIP
Curcumin
PC3
p50
VIP - + + -
curcumin - - + +
O.D. (Arbitrary Units)
20000
15000
10000
5000
0
*
++
Control
VIP
Curcumin+VIP
Curcumin

Figure 4

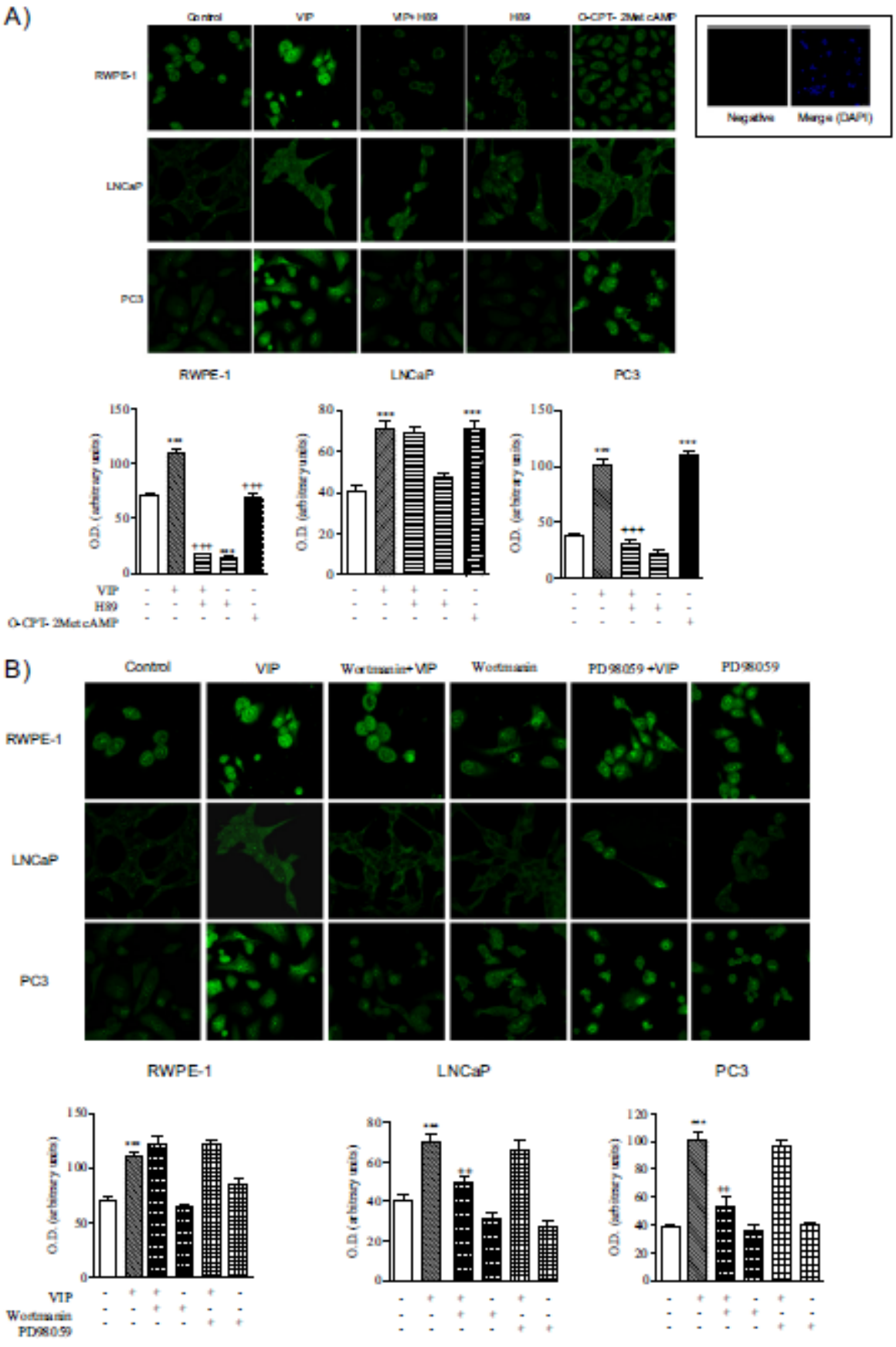
A)
Control
VIP
VIP+ H89
H89
O-CPT- 2Met cAMP
RWPE-1
LNCaP
PC3
Negative
Merge (DAPI)
RWPE-1
LNCaP
PC3
O.D. (arbitrary units)
VIP
H89
O-CPT- 2Met cAMP
B)
Control
VIP
Wortmanin→VIP
Wortmanin
PD98059→VIP
PD98059
RWPE-1
LNCaP
PC3
RWPE-1
LNCaP
PC3
O.D. (arbitrary units)
VIP
Wortmanin
PD98059

Figure 5

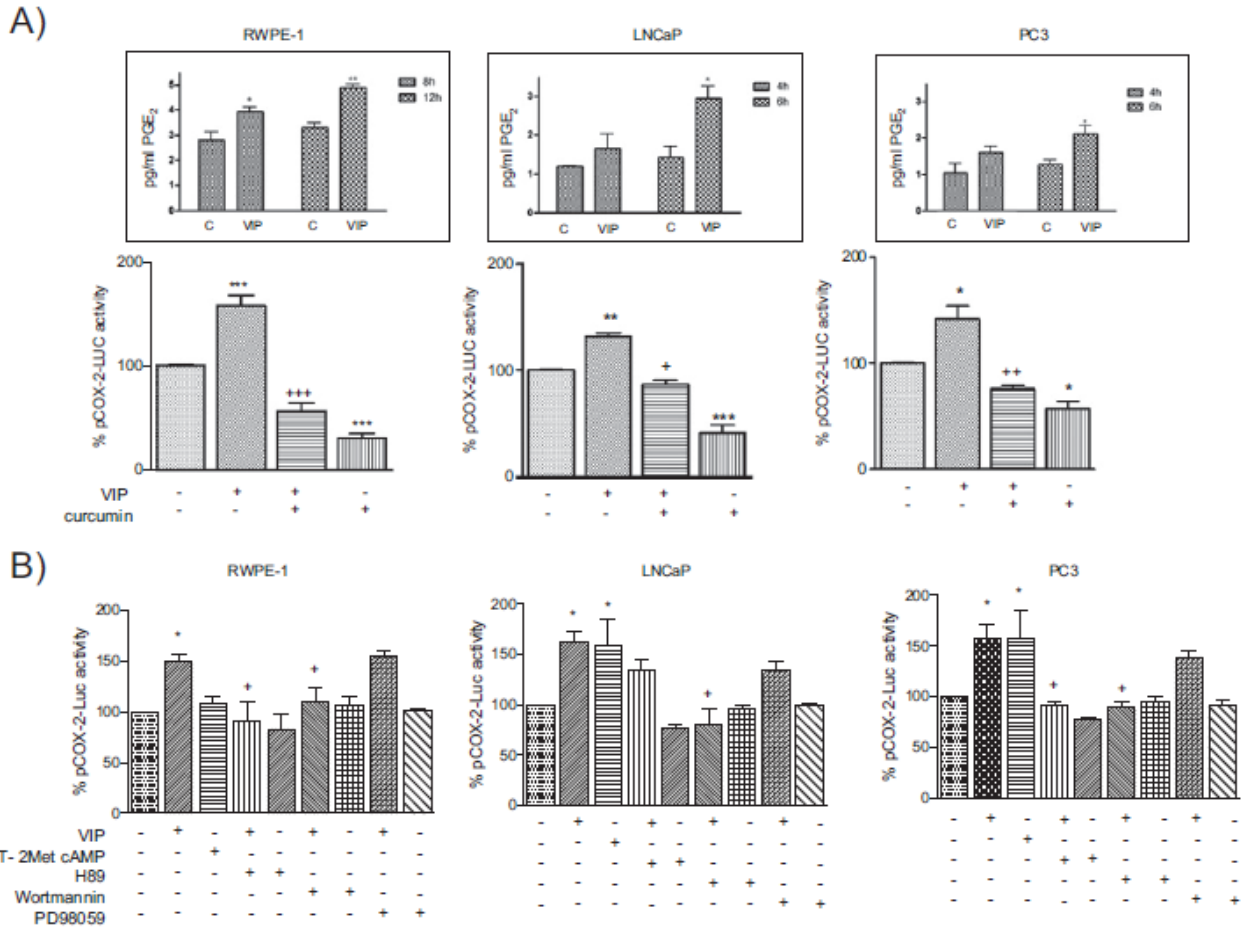
A)
RWPE-1
LNCaP
PC3
pg/ml PGE2
8h
12h
4h
6h
C
VIP
% pCOX-2-LUC activity
VIP
curcumin
B)
% pCOX-2-Luc activity
VIP
O-CPT- 2Met cAMP
H89
Wortmannin
PD98059

Figure 6

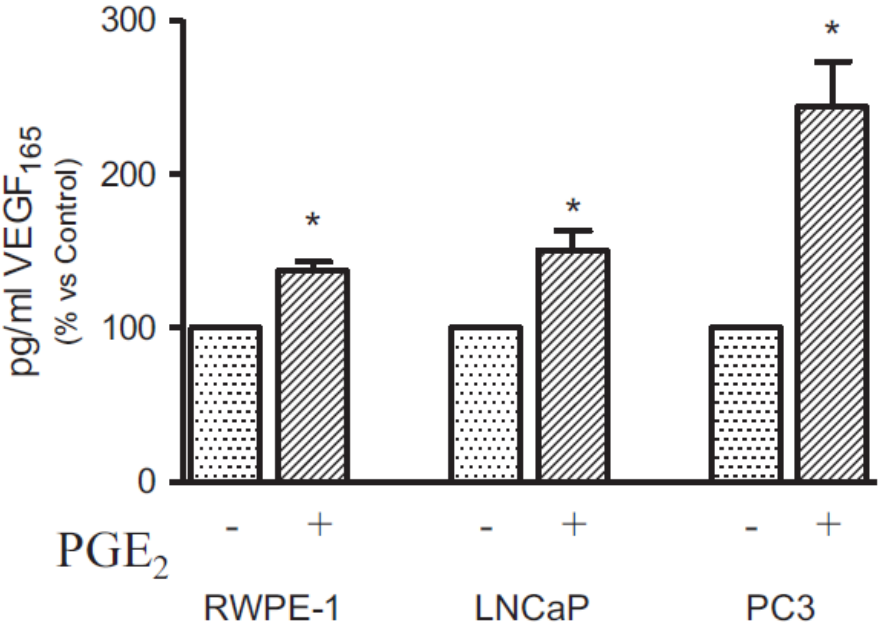

Figure 7

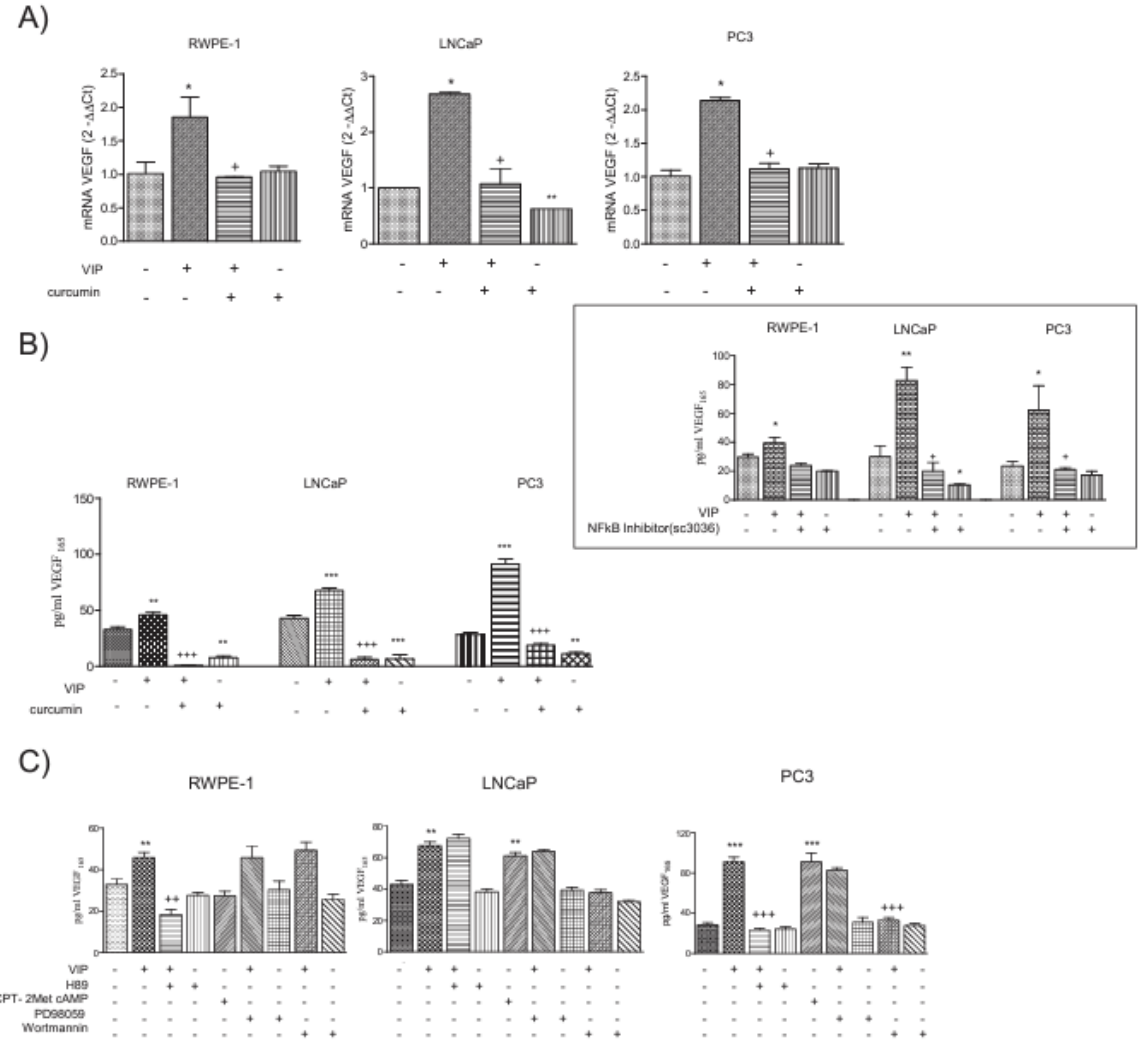
A)
RWPE-1
LNCaP
PC3
mRNA VEGF (2 -ΔΔCt)
VIP
curcumin
B)
RWPE-1
LNCaP
PC3
pg/ml VEGF165
VIP
curcumin
NFkB Inhibitor(sc3036)
C)
RWPE-1
LNCaP
PC3
VIP
H89
O-CPT- 2Met cAMP
PD98059
Wortmannin